Int. J. Solids Structures, 1978, Vol. 14, pp. 213–225. Pergamon Press. Printed in Great Britain

EFFECT OF STRAIN HARDENING ON THE LATERAL COMPRESSION OF TUBES BETWEEN RIGID PLATES

S. R. Reid and T. Yella Reddy

Engineering Department, University of Cambridge, Trumpington Street, Cambridge CB2 1PZ, England

(*Received* 11 *July* 1977; *received for publication* 27 *September* 1977)

Abstract—The lateral compression of circular tubes to large deformations is examined. The discrepancy between the theories and experiments reported previously is attributed in the main to an inadequate modelling of the stationary plastic hinges which are produced in the tube as it deforms. A model which utilises standard elastica theory is proposed which shows good agreement with the experimental data produced by the authors and that already published.

INTRODUCTION

The use of structural elements in impact energy absorbing systems has attracted a considerable amount of attention and several reviews of the literature exist[1–3]. Interest has centred on those metallic devices and structures which depend upon the absorption of energy by the production of plastic deformation.

As a step towards assessing the energy absorbing capacity of these devices under impact conditions their behaviour under quasi-static loading is usually first examined. Viewed generally as problems of plastic structural mechanics the analysis of such devices is formidable. Large geometry changes are usually produced and, in cases where tubular components are involved, the loading is seldom axisymmetric. However certain classes of problems have been examined both theoretically and experimentally with the aim of identifying the dominant features in the behaviour of particular types of structure as they deform.

McIvor *et al.*[4,5] and Miles[6] have considered the plastic collapse and subsequent deformation of general frames and, in particular, thin-walled beam structures. Their approach has been to incorporate experimentally determined constitutive equations for the localised zones of deformation which occur in such structures into large displacement framework analyses based on matrix methods. In contrast to this approach an experimental survey has been made of the large deformation of tubes subjected to a particular form of local loading[7, 8]. The aim of this was to gain an understanding of the local deformation modes in the zones referred to above.

The present authors have been concerned with the response of nests of tubes subjected to lateral compression between rigid plates[9]. In Ref. [9] it was demonstrated that the behaviour of an open system of tubes could be deduced simply from that of a single tube compressed between rigid plates. This latter problem has been examined previously in the literature[10–13]. DeRuntz and Hodge[11] proposed a theory based upon limit analysis which incorporated a geometrical stiffening effect reflecting the increase in load required to continue the deformation beyond initial collapse. The predicted rate of increase in the load however considerably underestimated that which was observed experimentally, the discrepancy increasing with deflection. It was concluded that the effects of strain hardening, which had been neglected by DeRuntz and Hodge, were significant. Redwood[12] pursued this point and confirmed that the experimental results given by DeRuntz and Hodge were typical. He referred to experiments performed by Burton and Craig[13] which also demonstrated a more rapid stiffening of the tube than that predicted by the DeRuntz and Hodge theory. Redwood attempted to incorporate the effects of strain hardening in a semi-empirical way but the results were not an appreciable improvement.

As far as the authors are aware this particular problem has not received attention since the publication of Redwood's note and it is therefore re-examined here. Since it is possible to envisage a number of similar situations in which stationary plastic hinges occur in conjunction with large deformations, it was thought useful to attempt to devise a method of incorporating the effects of strain-hardening in a more complete way into such problems.

It has been pointed out by McIvor *et al.*[5] that, in the application of structural plasticity to the type of problem envisaged above, the central issue is the post collapse load behaviour and not the determination of the collapse load itself which is principally the province of limit analysis. Solutions of structural problems involving large plastic deformation are not numerous. Problems involving beams and plates have been reviewed by Jones[14]. One of the main effects of "large" displacements (of the order of a few thicknesses) is to generate axial (for beams) or in-plane (for plates) forces which lead to considerable stiffening of the response to the applied loads. These solutions, which involve only moderately large displacements, are based upon a rigid–perfectly plastic or elastic–perfectly plastic material constitutive relationship.

For structural problems in which deformation is envisaged to occur through the action at plastic hinges leading to significant geometry changes the rate method first introduced by Batterman[15] would appear to provide the relevant theoretical starting point. Gürkök and Hopkins[16] have used this in the analysis of a pin-ended beam subjected to a uniformly distributed load. This is an axial force/bending interaction problem in which the rate method provides the conditions under which a central plastic hinge splits and is transformed into two parts which travel apart along the beam as the load is increased. Gill[17] has solved a similar problem without recourse to the formalism of the rate method. Onat and Shu[18] solved the problem of a circular arch subjected to an outward point load which tends to straighten it into a triangular shape. This involves truly large deflections and the main feature of their solution was again the occurrence of travelling hinges in the mode of deformation of the arch. Gill[19] has produced a novel solution of the same problem and also of the more complex case in which the circular arch is pulled through to a "*V*" shape using the concept of equivalent structures. Both of these analyses, which probably come closest to the problem under consideration, neglect the effect of strain hardening.

Onat[20] has pointed out that the rate method is inconclusive in problems involving plastic hinges when strain hardening is included and that to proceed one needs to consider the plastic regions which originate at the hinges and spread into the rigid portions. Onat[21] examined the effect of strain hardening on the stability of a simple frame after the limit load had been reached using a rigid–linearly strain hardening constitutive equation. The same approach is used here to provide an improved model for the behaviour of what, in the rigid plastic approximation, are plastic hinges at which large rotations occur. The results are compared qualitatively with the experiments reported by DeRuntz and Hodge[11] and in more detail with those described by Redwood[12] and also with a number performed by the authors. These latter were part of an extensive experimental investigation of a number of interesting features of the mode of deformation of single tubes which will be reported elsewhere.

MODES OF DEFORMATION AND RIGID–PERFECTLY PLASTIC SOLUTION

The problem considered is that of a circular tube of radius R and thickness t compressed between rigid, flat plates as shown in Fig. 1(a). It is assumed that the mode of deformation is two-dimensional and so the tube length enters the problem as a simple scaling factor; thus a tube of unit length is considered below. The effect of length dependent features of the mode of deformation will be discussed later. DeRuntz and Hodge proceeded to analyse the load–deflection relationship on the basis of a rigid–perfectly plastic theory assuming that the collapse mode consisted of four plastic line hinges as shown in Fig. 1(b). These hinges were assumed to remain stationary relative to the rigid portions of the tube, separation occurring from the outset between the tube and the plates in the centre of the contact zone. Burton and Craig proposed the alternative mode shown in Fig. 1(c) in which the tube is flattened in the contact zones and conforms to the shape of the plates throughout the loading. The contact zones terminate in hinges, V, which travel outwards as the deformation proceeds. The horizontal hinges H remain stationary relative to the tube as in the DeRuntz and Hodge model. Whilst both modes are valid from the point of view of limit analysis they clearly cannot both be correct vis á vis the observed behaviour of compressed tubes. A preliminary discussion of the relative merits of the two modes has been given in[9]. However, as far as the rigid–perfectly plastic solution is concerned it is shown below that the two modes imply identical load–deflection relationships and so an argument in favour of one or the other is superfluous. (One slight difference is that a

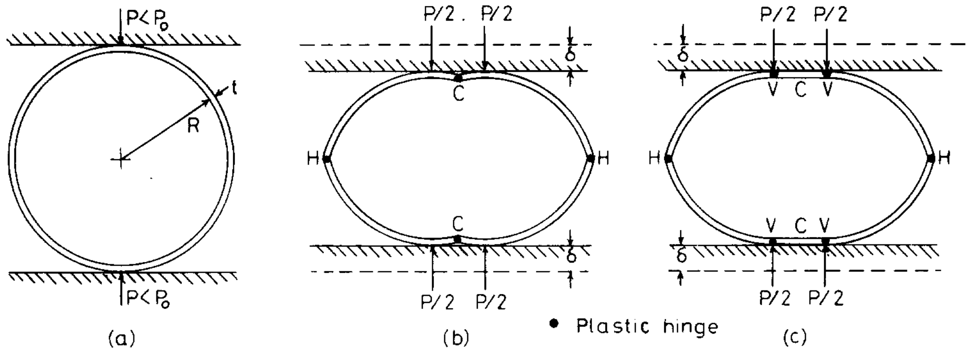

Fig. 1. (a) Undeformed tube geometry and loading arrangements; (b) DeRuntz and Hodge collapse mode; (c) Burton and Craig collapse mode.

change in mode is required in the DeRuntz and Hodge model when the two hinges on the vertical diameter meet whereas the Burton and Craig mode allows virtually complete collapse).

Figure 2 shows the system of forces and moments acting on one quadrant of the deforming tube which arise from considerations of equilibrium and symmetry. In Fig. 2(a) the quadrant is separated into a circular arc and a flat portion which is in a state of pure bending. In each case moment equilibrium implies that

$$\frac{PR}{2}\cos\beta = 2M_0 \qquad \text{or} \qquad P = \frac{4M_0}{R\cos\beta} \tag{1}$$

where, neglecting any interaction with shear and normal forces, $M_0 = \sigma_0 t^2/4$, σ_0 being the uniaxial yield stress.

Note that the moment arm of the external forces is $R \cos \beta$. Simple geometry gives

$$\delta = R\sin\beta \tag{2}$$

Thus

$$P = \frac{4M_0}{R(1-(\delta/R)^2)^{1/2}}. \tag{3}$$

Equation (3) clearly shows the necessity for the load to increase as the deflection increases this being due to the reduction in the moment arm.

Figure 3 shows the load–deflection characteristic given by Redwood for a 1.66 in radius annealed mild steel tube for which $t/R = 0.108$. The tube length was 4 in. The prediction of eqn (3) is shown together with the result obtained by Redwood after making some allowance for strain hardening. Redwood assumed rigid–linear strain hardening behaviour for the tube

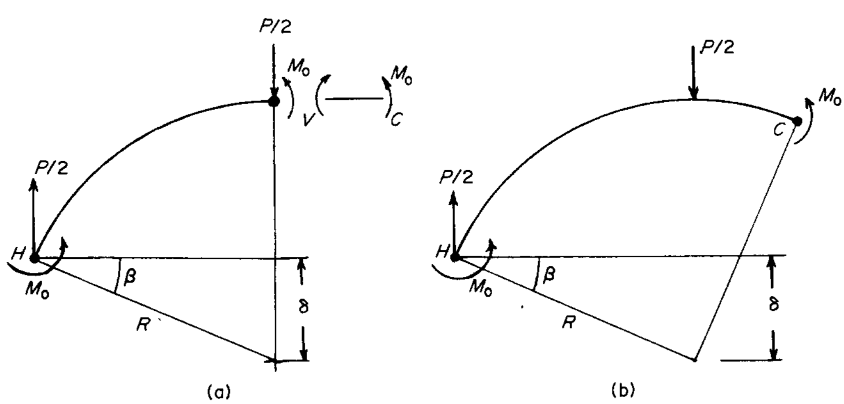

Fig. 2. System of forces and moments on a quadrant of the tube; (a) Burton and Craig mode; (b) DeRuntz and Hodge mode.

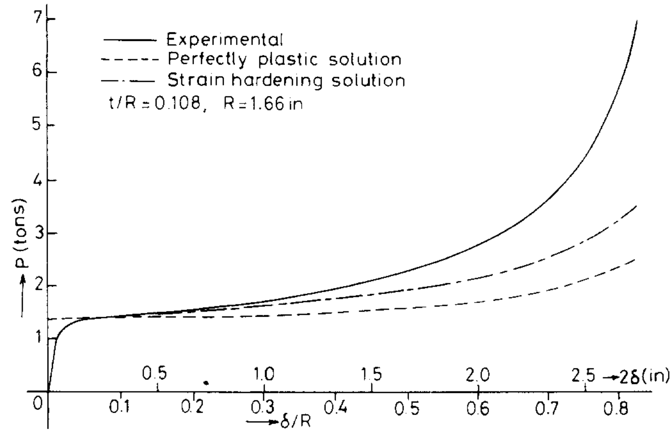

Fig. 3. Load-deflection graph for a mild steel tube $t/R = 0.108$, $R = 1.66$ in, $L = 4$ in from [12]

material and deduced the following modification of eqn (3)

$$P = \frac{4M_0}{R(1-(\delta/R)^2)^{1/2}}\left[1 + \frac{E_p}{3\sigma_0\alpha}\sin^{-1}(\delta/R)\right] \tag{4}$$

where E_p is the strain hardening modulus and α is a measure of the arc length of the region near to H in which the curvature change occurs. The arc length, s, is given by $s = \alpha t$ and a value of $\alpha = 5$ was used in obtaining the curve shown in Fig. 3. This value came from measurements on the specimens and implies a "hinge" length of approximately 0.9 in. Basically Redwood's method was equivalent to replacing eqn (1) by the following equation

$$\frac{PR}{2}\cos\beta = (M_0 + M_H) \tag{5}$$

and allowing M_H to increase with β in a manner determined by the hardening modulus E_p. It is clear from Fig. 3 that whilst this modification provides an improvement on DeRuntz and Hodge's theory it still falls short of the experimental data. This descrepancy was discussed at some length by Redwood and subsequently by DeRuntz and Hodge[12].

SECONDARY EFFECTS AND BASIS OF PROPOSED MODEL

In attempting to construct an improved model for the tube behaviour several secondary effects were considered. These included strain-hardening, the cause of the change in mode of deformation at $\delta/R \sim 0.3$ and the anticlastic curvature which is produced primarily in the flattened region near to the ends of the tube. A full consideration of all of these effects is beyond the scope of the present work, but details of an extensive series of experiments will be presented in a companion paper. However a significant experimental observation was that, as a tube was deformed the moment arm was noticeably less than that used in both eqns (1) and (5), the difference increasing with deflection. Furthermore, if $d(\delta)$ is the empirical moment arm corresponding to the deflection δ, it was found that replacing (1) by

$$P = \frac{4M_0}{d(\delta)} \tag{6}$$

produced significantly better agreement with the data. This led to the hypothesis that one of the main effects of strain hardening is in determining the geometry of the deforming tube and not simply in producing an increased moment M_H as assumed by Redwood.

In order to test this hypothesis the following theoretical model is proposed for a quadrant of the deforming tube.

(1) The material is considered to be rigid–linearly strain hardening. Thus the relationship between the change in curvature, κ and the moment at a particular section of the tube is

$$\kappa = \begin{Bmatrix} \dfrac{M - M_0}{E_p I} & M \geq M_0 \\ 0 & M < M_0 \end{Bmatrix} \tag{7}$$

where $I = t^3/12$ for a tube of unit length and thickness t.

(2) It is assumed that the structural elements of a quadrant of the tube are as shown in Fig. 4(a). The simple travelling hinge is retained at V as in Fig. 2(a). In principle this could be replaced by a strain hardening region in the manner described below. However the influence of the contact stress field on the behaviour of the hinge at V should also be considered in proposing such a replacement and this would seem to be too complex at this stage. Furthermore the tube profile appears to be reasonably circular as it passes through V, unlike the region around H in which there is a continuously changing curvature. Thus the portion of the tube not in contact with the plate is considered to be comprised of a rigid circular arc VB and a deformed circular arc BH. B denotes the extent of the hinge region around H and the bending moment there is M_0 as shown.

The basis of the method employed below is to determine a structure comprised of a rigid and a deformed portion, VB and BH respectively, the geometry of which can be determined for a given load factor $\lambda = P/P_0$ where $P_0 = 4(M_0/R)$. Large geometry changes are anticipated at the outset and consequently the analysis of the deformation from a circular arc to the arc BH must be capable of incorporating the effects of large deformations. Whilst VB undergoes large displacements from its position in the unloaded configuration, it is assumed to do so as a rigid body.

ANALYSIS OF THE ARC *BH*

Removing the horizontal rigid body translation of H, the deformed and undeformed configurations of BH are as shown in Fig. 4(b). Assuming that the centreline of the arc behaves inextensibly and taking the moment–curvature relationship given in eqn (7), it can be shown that the behaviour of BH is analogous to that of an elastica of flexural rigidity E_pI. The problem is esentially that of an *encastré* circular bar with a vertical end load, the governing equations for which can be found in the text by Frisch-Fay[22]. For completeness the equations and their solutions are given below although some of the details are omitted since they can be found in [22]; the same notation as [22] is employed for ease of reference.

Defining the deformed shape of BH by the intrinsic co-ordinates s, the arc length, and θ, the slope of the tangent, as shown in Fig. 4(b) and using eqn (7) the governing equation for a load $P/2$ is as follows

$$E_p I \frac{d^2\theta}{ds^2} = -\frac{P}{2}\sin\theta. \tag{8}$$

Defining $k^2 = (P/2E_pI)$ leads to

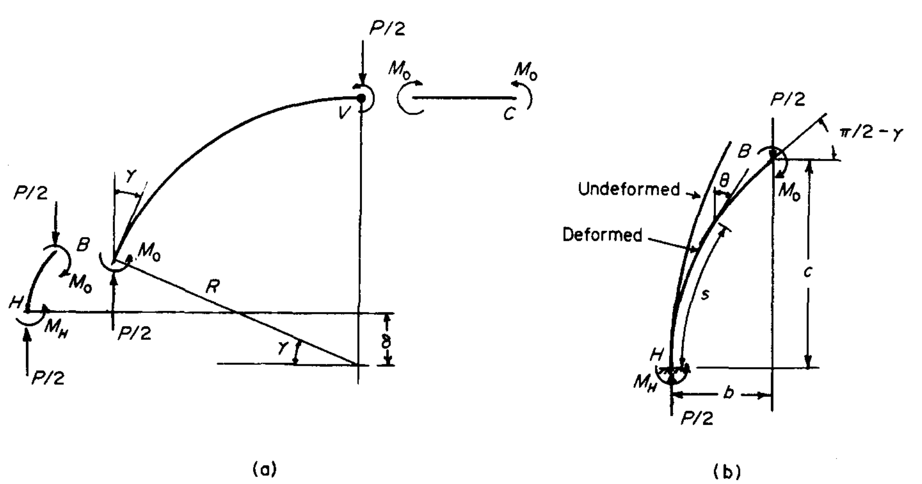

Fig. 4. (a) System of forces on quadrant of proposed model for tube collapse; (b) Deformation of *BH*

$$\frac{d^2\theta}{ds^2} = -k^2 \sin\theta. \tag{9}$$

Hence

$$\frac{1}{2}\left(\frac{d\theta}{ds}\right)^2 = k^2 \cos\theta + C \tag{10}$$

where C is a constant of integration.

If $\theta = \gamma$ at B then

$$\left(\frac{d\theta}{ds}\right)_{\theta=\gamma} = \frac{1}{R}. \tag{11}$$

Hence (10) becomes

$$\frac{1}{2}\left(\frac{d\theta}{ds}\right)^2 = k^2(\cos\theta - \cos\gamma) + \frac{1}{2R^2}. \tag{12}$$

At end H, $M_H = M_0 + (Pb/2)$

$$\therefore M_H - M_0 = E_p I\left[\left(\frac{d\theta}{ds}\right)_{\theta=0} - \frac{1}{R}\right]$$

$$\therefore \left(\frac{d\theta}{ds}\right)_{\theta=0} = \frac{1}{R} + k^2 b. \tag{13}$$

From (12) and (13), the parameter b satisfies the following quadratic equation

$$(b/R)^2 + (b/R)\frac{2}{k^2R^2} - \frac{2}{k^2R^2}(1-\cos\gamma) = 0. \tag{14}$$

In [22] the subsidiary variables α, ϕ and p are introduced where

$$\left.\begin{aligned} \cos\alpha &= \cos\gamma - \frac{1}{2k^2R^2} \\ \text{and} \quad 1-\cos\theta &= 2p^2\sin^2\phi = (1-\cos\alpha)\sin^2\phi \end{aligned}\right\}. \tag{15}$$

Thus

$$\cos\alpha = 1 - 2p^2 \tag{16}$$

The main geometrical parameter required for the tube analysis is c (shown in Fig. 4b). This is given in [22] by

$$c = [2E(p,\phi_1) - F(p,\phi_1)]/k \tag{17}$$

where $\phi = \phi_1$ corresponds to $\theta = \gamma$ and F and E are the incomplete elliptic integrals of the first and second kind respectively. If $l/2$ is the length of BH (half the "hinge" length) then it can be shown that

$$l = 2F(p,\phi_1)/k. \tag{18}$$

The final results required from [22] come from eqns (15) and (16). Since $\phi = \phi_1$ corresponds to $\theta = \gamma$ we have

$$\cos\gamma = 1 - 2p^2 + \frac{1}{2k^2R^2} \tag{19}$$

and

$$\phi_1 = \cos^{-1}\left(\frac{1}{2pkR}\right). \tag{20}$$

SYSTEM OF EQUATIONS GOVERNING TUBE COMPRESSION

The method by which the equations above provide a relationship between P and δ will now be described. Basically one specifies a value of P and then calculates the geometrical parameters sequentially. To do this the equations from the previous section are supplemented by the following two equations which are derived from Fig. 4(a) by equilibrium and geometrical considerations

$$P = \frac{4M_0}{R\cos\gamma}$$

$$\delta = R\sin\gamma - c. \tag{21}$$

Using the load parameter λ and taking $P_0 = (4M_0/R) = (\sigma_0 t^2/R)$ we have

$$k = m\surd(\lambda) \tag{22}$$

where

$$m = \left(\frac{6\sigma_0}{E_p tR}\right)^{1/2}. \tag{23}$$

A non-dimensional parameter which plays an important role in the solution is mR. The steps by which λ is related to δ/R are as follows:—

$\lambda \to \gamma$: from (21) $\quad \cos\gamma = \dfrac{4M_0}{PR} = \dfrac{P_0}{P} = \dfrac{1}{\lambda}$

$$\cos\gamma = 1/\lambda \tag{I}$$

$\lambda, \gamma \to p$: from (19), (23), (I) $\quad 2p^2 = 1 - \dfrac{1}{\lambda}\left(1 - \dfrac{1}{2m^2R^2}\right)$

or

$$p = \frac{1}{\surd 2}(1 - n/\lambda)^{1/2} \tag{II}$$

where

$$n = 1 - \frac{1}{2m^2R^2}$$

$p \to \phi_1$: from (20) $\quad \phi_1 = \cos^{-1}\left(\dfrac{1}{2pmR\surd(\lambda)}\right)$ (III)

$p, \phi_1 \to c/R$: from (17) $\quad c/R = [2E(p,\phi_1) - F(p,\phi_1)]/mR\surd(\lambda)$ (IV)

$\gamma, c/R \to \delta/R$: from (22) $\quad \delta/R = \sin\gamma - c/R$ (V)

Thus one can produce a dimensionless load–deflection plot (i.e. λ vs δ/R) using eqn (I)–(V).

Furthermore the parameters b and l can be determined from (14) and (18) if required.

RESULTS AND COMPARISON WITH EXPERIMENTS

In order to derive results from the theory, values of σ_0 and E_p are required. In his discussion of the results obtained by Burton and Craig for a 3.32 in diameter annealed mild steel tube, Redwood included the stress–strain graph reproduced in Fig. 5 from which he deduced values of 18 ton/in^2 (4×10^4 lbf/in^2) and 92 ton/in^2 (20×10^4 lbf/in^2) for σ_0 and E_p respectively. The value for σ_0 correlates well with the measured value of approximately 1.4 ton for P_0. Although Redwood claimed that the value of E_p should over-estimate the effect of strain hardening it is clear that in fact it gives a reasonable mean strain hardening modulus for the annealed tubes. The result of using the two values quoted for σ_0 and E_p in the theory is shown in Fig. 6.

A quantitative comparison with the experiments performed by DeRuntz and Hodge is not possible. They tested as-received tubes and gave no other specification than that they were made from mild steel. The values of P_0 given in their paper for 0.18 in and 0.12 in thick tubes imply a value of approximately 6.5×10^4 lbf/in^2. This clearly indicates that the tubes had been heavily worked during their manufacture. This value is above the U.T.S. of the mild steel used by Burton and Craig and also that used by the authors. It can be shown that reasonable agreement between their experiments and the theory occurs with a value of 13×10^4 lbf/in^2 for E_p. Such a value is not unreasonable for the tangent modulus of mild steel strain hardened under uniaxial load. However in view of the lack of information about the material used by DeRuntz and Hodge no more than qualitative agreement between the theory and their results can be claimed.

Compression tests were performed by the authors on an annealed 2 in diameter tube and a partially annealed 3 in diameter tube both of which had a wall thickness of 0.064 in. and a length of 6 in. The resulting experimental and theoretical load–deflection graphs are shown in Fig. 7. The material stress–strain characteristic is shown in Fig. 8 from which a value of 24×10^4 lbf/in^2 was deduced for E_p. The values of σ_0 taken for the 2 in and 3 in tubes were 3.9×10^4 lbf/in^2 and 4.7×10^4 lbf/in^2 respectively. These values are consistent with the values of P_0 for the two tubes and measurements of the Vickers Hardness Number which were made.

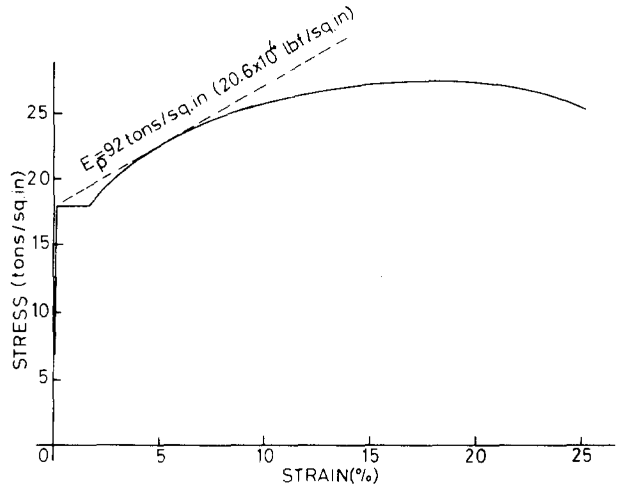

Fig. 5. Stress–strain curve for mild steel from [12].

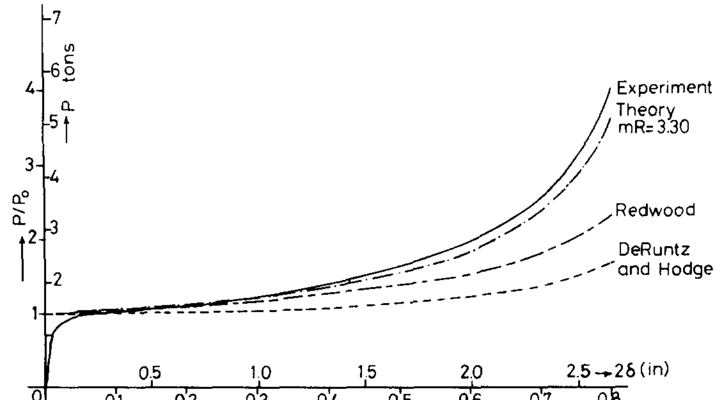

Fig. 6. Comparison between theory and experiment for data given by Redwood.

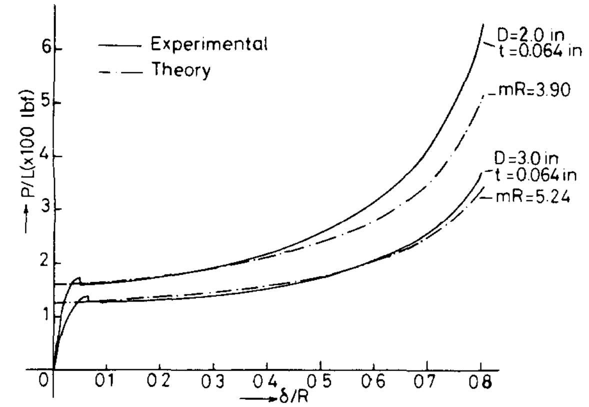

Fig. 7. Experimental and theoretical load-deflection traces for 2 in. and 3 in. diameter mild steel tubes.

Table 1 shows the sequence of computed values of the parameters which led to the results shown in Fig. 6. As well as the loads and corresponding deflections, the value of the change in curvature at H (Fig. 4a), which is given by k^2b from eqn (13), is included together with the length of the hinge calculated using eqn (18). The last column indicates that the "hinge" length increases from zero to a maximum value of about 1.1 in and then reduces to approximately 0.8 in at a δ/R value of 0.8. This behaviour points to an important feature of the mode of deformation but also implies an inaccuracy in the method both of which will be discussed in the next section. It is interesting to note that the average value of the theoretical hinge length is approximately 0.9 in which compares well with the value of 0.9 in indicated by Redwood. This is given with the corresponding values for the 2 in and 3 in tubes in Table 2.

DISCUSSION

Explanation of the more rapid increase in tube stiffness at large deflections

The theory used is based upon a relatively crude representation for the material behaviour. In particular the choice of a suitable value for the hardening modulus E_p is somewhat arbitrary although the values chosen in the applications above represent reasonably well defined mean values for the tangent modulus over a range of strains. No doubt more refined techniques could be devised in which the strain range at H could be used to define a more accurate value of E_p iteratively in conjunction with the stress–strain relationship. In spite of this the agreement with the experiments quoted is encouraging.

Of greatest interest is the ability of the theory to model the tendency of the slope of the load-deflection curve to increase more rapidly in the later stages of the deformation. An explanation of the source of this can be found by examining the results for a typical case. Consider the results given in Table 1. The variations in the curvature at H and in the length of

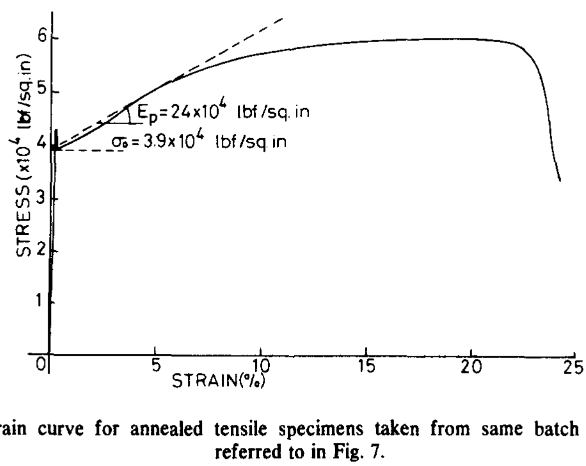

Fig. 8. Stress–strain curve for annealed tensile specimens taken from same batch of mild-steel tube referred to in Fig. 7.

Table 1. Theoretical data for Redwood's mild steel tube

Load (tons)	Deflection (in)	Change in curvature at H (in^{-1})	Length of hinge (in)
1.39	0.00	0.00	0.00
1.53	0.47	0.47	0.94
1.67	0.86	0.79	1.05
1.81	1.14	1.05	1.08
1.95	1.37	1.27	1.09
2.08	1.54	1.47	1.09
2.22	1.69	1.66	1.08
2.36	1.81	1.83	1.07
2.50*	1.92	1.98	1.06
2.64	2.01	2.13	1.04
2.78	2.08	2.27	1.03
2.92	2.15	2.41	1.02
3.06	2.21	2.54	1.00
3.20	2.26	2.66	0.99
3.34	2.31	2.78	0.97
3.47	2.35	2.89	0.96
3.61	2.39	3.00	0.95
3.75	2.43	3.11	0.94
3.89	2.46	3.22	0.93
4.03	2.49	3.32	0.91
4.17	2.52	3.42	0.90
4.31	2.54	3.52	0.89
4.45	2.57	3.61	0.88
4.59	2.59	3.70	0.87
4.73	2.61	3.79	0.86
4.86	2.63	3.88	0.85
5.00	2.64	3.97	0.84
5.14	2.66	4.06	0.83

Table 2. Comparison of hinge lengths

Tube	Length of hinge	
	Experiments	Theory
Authors' 2 in diameter mild steel	0.49 in (δ/R = 0.83)	0.50 in (mean) 0.45 in (δ/R = 0.81)
Authors' 3 in diameter	0.65 in (δ/R = 0.67) 0.46 in (δ/R = 0.8)	0.59 in (mean) 0.64 in (δ/R = 0.66) 0.56 in (δ/R = 0.8)
Redwood's 3.32 in diameter mild steel	0.9 in (mean)	0.94 in (mean)

the hinge are shown in Fig. 9. As the load increases from P_0 the zone over which plastic deformation occurs expands rapidly, the change in curvature at H increasing almost linearly. In this first phase therefore the effect of strain hardening is predominantly to disperse the deformation over a significant arc of the cross-section of the tube in contrast to the production of a localised hinge as assumed in limit analysis. The hinge reaches its maximum length at a deflection ratio $\delta/R \approx 0.4$ and subsequently reduces. As a consequence of this the rate of change of curvature with deflection begins to increase. This causes a more rapid increase in the moment at H which in turn contributes to the more rapid rise in the applied load. It is interesting to note that the curvature change takes on an even greater rate of increase around $\delta/R \approx 0.6$. It has previously been reported[9] that noticeable changes in the character of the load–deflection curve occur around the two values indicated above and these results would lead one to suggest that these changes correspond to the characteristics shown in Fig. 9.

The reduction in the length of HB, whilst an important feature of the model, does indicate a certain degree of approximation in the method. As outlined above, the determination of the deflection for a given load factor is a self-contained process, there being no explicit dependence on the loading history. The tendency of the length of the plastic region BH to decrease shows that this cannot be the case. This behaviour indicates that a small part of the tube experiences a reduction in bending moment. Neglecting any interaction between bending and shear or normal force components (implicit in our assumptions of inextensibility and eqn 7) this implies a degree of unloading in certain parts of the tube. Since the external loads are increasing monotonically it is expected that the significance of this unloading will be small†. One consequence of this feature of the solution is that VB will not be completely circular as assumed since part of it adjacent to B will have a radius of curvature less than R due to its previous history of plastic bending. The non-circular part of VB is that which has undergone least change of curvature in BH and so its neglect should not be significant.

The changes in the length of the plastic zone revealed by the theory are physically reasonable. The arc VH is in a state of contraflexure and, as the deformation proceeds, is reducing in the length. It might therefore be expected (and indeed it can be clearly seen in many tests) that the zone of most intense bending near to H becomes more concentrated.

Importance of $mR = (6\sigma_0 R/E_p t)^{1/2}$

The response of a tube at large deflections is principally determined by the magnitude of the parameter mR. The smaller the value of mR the bigger is the deviation from the DeRuntz and Hodge theory which corresponds to $mR \to \infty$. This is shown clearly in the family of non-dimensional load–deflection curves given in Fig. 10. The values of mR for the specific tests shown in Figs. 6 and 7 have been included on those figures.

It is interesting to note that mR consists of a combination of material and geometric variables. Thorton and Magee[24] have recently discussed the dependence of the energy absorbing capacity of a material on the geometry of the testing mode. In particular they compared the performance of tubes of different materials in uniaxial tension and compression and concluded that, because of the differences in the modes of deformation, different material parameters are significant in different modes. They found that in tension the ultimate tensile strength, σ_{ult}, and the uniform elongation (i.e. tensile strain to fracture), ϵ_u, were significant whilst the latter was unimportant in axial compression. The results above would seem to indicate that for lateral compression σ_0/E_p plays a significant role. (This assumes that ϵ_u is sufficiently large to preclude formation of cracks at the hinges H as discussed in [9]).

Influence of secondary effects

Finally it should be noted that some of the secondary effects mentioned in an earlier section may have a noticeable effect on the load–deflection curves. It has been observed[9] that

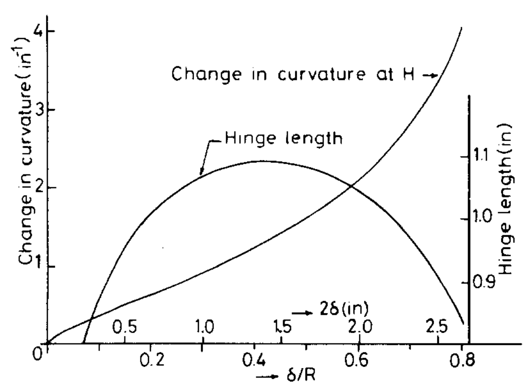

Fig. 9. Variation in the length of the hinge around H and curvature change at H with δ/R.

†The situation is somewhat similar to that discussed by Horne[23] in his treatment of the elastic–plastic theory of compression members.

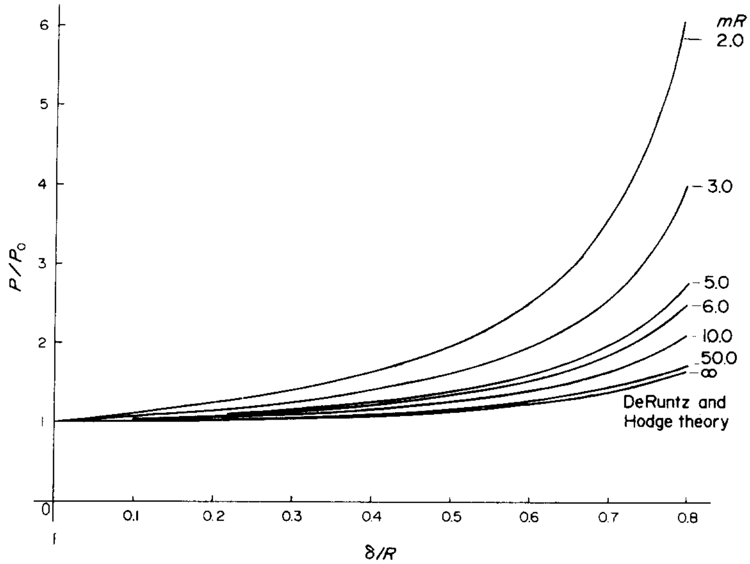

Fig. 10. Influence of mR on large deflection response of tubes.

separation occurs within the contact zone to a degree which depends to a certain extent on the material used. Whilst not being as large as that predicted by the DeRuntz and Hodge mode of deformation, its occurence does imply an increase in the curvature change within the "contact" region which, because of strain hardening, would qualitatively require an increase in the applied load. Similarly anticlastic curvature in the end regions of the tube will lead one to expect an increase in the applied load in excess of that calculated using the theory above. Either (or both) of these effects could account for the tendency in Figs. 6 and 7 for the theory to fall below the experimental curves for δ/R approaching 0.8. These points will be discussed in the companion paper referred to earlier. It is the authors' opinion however that the predominant features of the large deformation behaviour of laterally compressed tubes can be accounted for using the treatment of the stationary hinges described above.

CONCLUSION

It is accepted that the neglect of strain hardening is a reasonable approximation in situations in which geometry changes affect the major load carrying mechanism, (provided that thereafter the in-plane strains are not excessive.) However, when the mode of deformation consists principally of bending and no in-plane forces are developed or where their effects are minimal, the neglect of strain hardening can lead to substantial errors. These are due not only to the strengthening of the material in the regions of plastic deformation but also to the influence that this strengthening imposes on the geometry of the mode of deformation of the structure. In these latter cases a model of the plastic regions is called for which is an improvement on the concept of a plastic hinge. This has been attempted in the present paper and, with reference to the specific problem considered, it would appear that the theory provides a better prediction of the load–deflection characteristic of the structure as well as an insight into the manner in which strain-hardening influences the response. Furthermore the predictions of the extent of the plastic zone correlate well with experimental data.

From Fig. 10 it is clear that the parameter mR is important in determining the large deformation response of a tube. Within the approximations of the theory, it would seem that one could maximise the energy absorbing capacity of tubes of a given material by choosing the geometrical parameters in such a way as to minimise mR.

REFERENCES

1. A. A. Ezra, Program for the exploitation of unused NASA patents. *Ann. Rep.*, NASA-CR-106648, (June 1968).
2. A. A. Ezra and R. J. Fay, An assessment of energy absorbing devices for prospective use in aircraft impact situations. *Dynamic Behaviour of Structures* (Edited by G. Herrman and N. Perrone), p. 225. Pergamon Press, Oxford, (1972).
3. B. Rawlings, *Response of structures to dynamic loads. Proc. Conf. on Mechanical Properties of Materials at High Rates of Strain*, pp. 279–298. Institute of Physics, (1974).

4. I. K. McIvor, W. J. Anderson and M. Bijak-Zochowski, An experimental study of the large deformation of plastic hinges. *Int. J. Solids Structures.* **13**, 53–61 (1977).
5. I. K. McIvor, A. S. Wineman and H. C. Wang, Plastic collapse of general frames. *Int. J. Solids Structures.* **13**, 197–210 (1977).
6. J. C. Miles, The determination of collapse load and energy absorbing properties of thin walled beam structures using matrix methods of analysis. *Int. J. Mech. Sci.* **18**, 399–405 (1976).
7. A. R. Watson, S. R. Reid, W. Johnson and S. G. Thomas, Large deformations of thin-walled circular tubes under transverse loading II. *Int. J. Mech. Sci.* **18**, 387–397 (1976).
8. A. R. Watson, S. R. Reid and W. Johnson, Large deformations of thin-walled circular tubes under transverse loading—III. *Int. J. Mech. Sci.* **18**, 501–509 (1976).
9. W. Johnson, S. R. Reid and T. Y. Reddy, The compression of crossed layers of thin tubes. *Int. J. Mech. Sci.* **19**, 423 (1977).
10. L. D. Mutchler, Energy absorption of aluminium tubing. *J. Appl. Mech.* **27**, 740–743 (1960).
11. J. A. DeRuntz and P. G. Hodge, Crushing of a tube between rigid plates. *J. Appl. Mech.* **30**, 391–395 (1963).
12. R. G. Redwood, Discussion of Ref. 11. *J. Appl. Mech.* **31**, 357–358 (1964).
13. R. H. Burton and J. M. Craig, An investigation into the energy absorbing properties of metal tubes loaded in the transverse direction. B.Sc (Eng) Report, University of Bristol, Bristol, England (1963).
14. N. Jones, Review of the plastic behaviour of beams and plates. *Int. Shipbuilding Progr.* **19**, 313–327 (1972).
15. S. C. Batterman, On the rate equations for plane curved beams. *J. Appl. Mech.* **34**, 500–503 (1967).
16. A. Gürkök and H. G. Hopkins, The effect of geometry changes on the load carrying capacity of beams under transverse load. *SIAM* **25**, 500–521 (1973).
17. S. S. Gill, Effect of deflexion on the plastic collapse of beams with distributed load. *Int. J. Mech. Sci.* **15**, 465–471 (1973).
18. E. T. Onat and L. S. Shu, Finite deformations of a large rigid perfectly plastic arch. *J. Appl. Mech.* **29**, 549–553 (1962).
19. S. S. Gill, Large defection rigid plastic analysis of a built-in semi-circular arch. *Int. J. Mech. Engng Ed.* **4**, 339–355 (1976).
20. E. T. Onat, The influence of geometry changes on the load-deformation behaviour of plastic solids. *Plasticity* (Edited by E. H. Lee and P. S. Symonds), pp. 225–238. Pergamon Press, Oxford (1960).
21. E. T. Onat, On certain second-order effects in the limit design of frames. *J. Aero. Sci.* **22**, 681–684 (1955).
22. R. Frisch-Fay, *Flexible Bars.* Butterworths, London (1962).
23. M. R. Horne, The elastic-plastic theory of compression members. *J. Mech. Phys. Solids.* **4**, 104–120 (1956).
24. P. H. Thornton and C. L. Magee, The interplay of geometric and materials variables in energy absorption. *J. Engng Mat. Tech.* **99**, 114–120 (1977).